

# Graph Representation Learning Strategies for Omics Data: A Case Study on Parkinson’s Disease

Elisa Gómez de Lope\*  
Department of Engineering  
University of Luxembourg  
elisa.gomezdelope@uni.lu

Saurabh Deshpande  
Department of Engineering  
University of Luxembourg  
saurabh.deshpande@uni.lu

Ramón Viñas Torné  
Dept. of Computer and Communication Sciences  
École polytechnique fédérale de Lausanne (EPFL)  
ramon.vinastorne@epfl.ch

Pietro Liò  
Department of Computer Science  
University of Cambridge  
pl219@cam.ac.uk

Enrico Glaab<sup>1</sup>  
Luxembourg Center for Systems Biomedicine  
University of Luxembourg  
enrico.glaab@uni.lu

Stéphane P. A. Bordas  
Department of Engineering  
University of Luxembourg  
stephane.bordas@uni.lu

**Abstract**—Omics data analysis is crucial for studying complex diseases, but its high dimensionality and heterogeneity challenge classical statistical and machine learning methods. Graph neural networks have emerged as promising alternatives, yet the optimal strategies for their design and optimization in real-world biomedical challenges remain unclear. This study evaluates various graph representation learning models for case-control classification using high-throughput biological data from Parkinson’s disease and control samples. We compare topologies derived from sample similarity networks and molecular interaction networks, including protein-protein and metabolite-metabolite interactions (PPI, MMI). Graph Convolutional Network (GCNs), Chebyshev spectral graph convolution (ChebyNet), and Graph Attention Network (GAT), are evaluated alongside advanced architectures like graph transformers, the graph U-net, and simpler models like multilayer perceptron (MLP).

These models are systematically applied to transcriptomics and metabolomics data independently. Our comparative analysis highlights the benefits and limitations of various architectures in extracting patterns from omics data, paving the way for more accurate and interpretable models in biomedical research.

**Index Terms**—Graph neural networks, transformers, machine learning, omics, transcriptomics, metabolomics, Parkinson’s disease

## I. INTRODUCTION

Analyzing omics data in complex diseases like Parkinson’s disease (PD) is challenging due to high dimensionality, noise, heterogeneity, and typically small sample sizes. Recently, graph representation learning methods combining machine learning and graph theory, have reported potential in tackling these challenges by exploring relational information and capturing structural and functional interactions [1]–[4]. Graph Neural Networks (GNNs) propagate feature information through graph structures, making them particularly well-suited for biomedical data where complex interrelationships can be intuitively represented as networks.

Previous work, such as that of Chereda et al. [5], [6], has used GNNs to predict disease outcomes using a PPI network. Other approaches have mapped multi-omics data into patient similarity networks [7]–[9], but acquiring such data from the same cohort is often impractical for PD [10]. Our study aims to address this gap by comparing different graph representation learning methods to identify patterns within individual omics data in PD. The findings may guide future research in modeling omics data and uncover fingerprints relevant to PD, contributing to a deeper understanding of its pathology.

## II. MATERIALS AND METHODS

### A. Datasets

Both sample similarity and molecular interaction networks modelling pipelines were trained and evaluated in two independent cohorts: PPMI (whole blood transcriptomics) [11] and LUXPARK (blood plasma metabolomics) [12]. After the pre-processing steps described in Appendix A, the PPMI dataset contained 14,548 gene expression features for 378 samples (189 controls and 189 PD patients), while the LUXPARK set contained 1,079 metabolite profiles for 1,136 subjects (590 controls and 546 PD patients). Pre-processing of metabolomics data only partially mitigated the medication effect, potentially obscuring the biological interpretation of the results from LUXPARK data.

### B. Modelling Sample Similarity Networks

Sample-sample similarity networks are an emerging paradigm in modelling omics data [7]–[9]. Here, an end-to-end modeling pipeline was developed, trained, and evaluated in a 10-fold cross-validation for PD case-control node classification on LUXPARK (metabolomics) and PPMI (transcriptomics) data. The pipeline includes 5 steps: data scaling, feature selection with LASSO [14], building a sample-sample similarity graph, the formulation of the GNN model for the binary node classification task, and a post-hoc explainer module using GNN-Explainer [15] (see schema in Figure 1 of Appendix B).

The topology of the network is defined with an adjacency matrix  $A$ , which is constructed by finding pairwise cosine similarity scores among samples that are larger than a threshold hyperparameter  $s$  (eq. 2) [16]:

$$\text{cosine similarity}(i, j) = cs(x_i, x_j) = \cos(\theta) = \frac{x_i \cdot x_j}{\|x_i\|_2 \|x_j\|_2} \quad (1)$$

where  $\|x_i\|_2$  is the 2-norm of the feature vector  $x_i$  of sample  $i$ .

$$A_{ij} = \begin{cases} cs(x_i, x_j), & \text{if } i \neq j \text{ and } cs(x_i, x_j) \geq s \\ 0, & \text{otherwise} \end{cases} \quad (2)$$

### C. Modelling Molecular Interactions Networks

Molecular interaction networks represent relationships between molecular entities. A modeling pipeline based on graph representation learning was implemented to classify PD cases and controls mapping a PPI on the transcriptomics data from PPMI, and a MMI on the metabolomics data from LUXPARK independently. The pipeline includes several steps: constructing the PPI from STRING (v12.0) [17], or MMI from STITCH (v5.0)

\*Corresponding author. Email: elisa.gomezdelope@uni.lu  
<sup>1</sup> On behalf of the NCER-PD Consortium

[14], adjusting the feature matrix of omics profiles  $X$  to include only molecules represented in the network, scaling the data, formulating the GNN model as a binary graph classification task, and analyzing explainability with GNN-Explainer (a schema is available in Figure 2 of Appendix B).

Notably, not all transcriptomics and metabolomics features mapped to the PPI and MMI, respectively. In PPMI, the final graph  $G = (E, V)$  included 5,848 nodes, and the feature matrix  $X$  was adjusted accordingly. The MMI network for LUXPARK included only 474 vertices (44% of the initial feature set), despite efforts in matching features via multiple chemical identifiers including PubChem, KEGG, ChEBI, CAS, SMILES and inchikeys.

#### D. Comparative analysis and evaluation

We evaluated the performance of several models, including GCN, ChebyNet, and GAT, applied to molecular interaction networks (graph classification) and sample similarity networks (node classification) for PD vs. control classification on PPMI and LUXPARK datasets. Their performance was also compared against that of an MLP [18], considering factors like feature selection and model depth. Additionally, we assessed the performance of various state-of-the-art GNN and transformer-based approaches, including Graph U-Net [19] and graph transformers (GPST [20], GTC [21]). Finally, the models were compared with similarity-based versus random edges.

Unless specifically mentioned, all models use 2 layers of their respective transformation followed by ReLU activation [22].

### III. RESULTS AND DISCUSSION

#### A. Sample similarity versus molecular interaction networks

We compared the performance of GCN, ChebyNet, and GAT models in the two modeling pipelines: using sample similarity networks (SSNs) and molecular interaction networks (MINs). We found that SSNs consistently outperformed MINs, particularly in the LUXPARK dataset. We hypothesize that this discrepancy is attributed to the incompleteness of MINs, especially that of metabolite-metabolite interactions, and the potential irrelevance of healthy individual-based MINs to PD pathology.

#### B. The power of the graph structure: MLP vs GNNs

GNNs generally outperformed the MLP, indicating that GNNs can more effectively integrate information, capturing complex dependencies and interactions in the omics profiles that the MLP might miss.

#### C. The effect of feature selection and depth of the network

The ablation experiments show that the incorporation of LASSO-based feature selection consistently improved model performance, addressing the challenge of modeling high-dimensional high-throughput biological data with limited sample sizes.

Increasing the number of layers did not improve model performance, likely due to overfitting given the limited sample size.

#### D. Transformers generally outperform traditional GNNs

The graph transformer architectures studied here showed higher average cross-validated performance than "traditional" GNN layers (GCN, GAT, Chebyshev) in both datasets. Among traditional layers, *ChebyNet* showed slightly higher performance. Other architectures like Graph U-Net generally underperformed compared to traditional GNNs. Graph transformers seem to be more expressive, leveraging the sample-similarity through the edge attributes.

#### E. Inductive biases: similarity-based versus random edges

In PPMI, models with similarity-based edges reported higher performance metrics than those with random edges. Graph transformers were less sensitive to edge type, likely due to their ability to infer these nuances through the attention mechanism. In LUXPARK, models performed comparably regardless of edge type, suggesting that larger sample size may reduce the need for inductive biases. Additionally, sparser networks like SSNs may limit the flow of information and hinder learning rich embeddings.

TABLE I: Cross-validated performance for molecular interaction networks in PPMI and LUXPARK.

	PPI network (PPMI)		MMI network (LUXPARK)	
	AUC	F1	AUC	F1
ChebyNet	0.47 ± 0.08	0.38 ± 0.29	0.54 ± 0.07	0.36 ± 0.26
GCN	0.52 ± 0.05	0.48 ± 0.28	0.48 ± 0.07	0.39 ± 0.14
GAT	0.54 ± 0.04	0.52 ± 0.22	0.55 ± 0.06	0.52 ± 0.05

TABLE II: Cross-validated performance for sample similarity networks in PPMI and LUXPARK.

	PPMI		LUXPARK	
	AUC	F1	AUC	F1
ChebyNet	<b>0.58 ± 0.08</b>	0.52 ± 0.18	<b>0.83 ± 0.05</b>	<b>0.73 ± 0.06</b>
GAT	0.56 ± 0.07	<b>0.55 ± 0.06</b>	0.79 ± 0.04	0.71 ± 0.05
GCN	0.56 ± 0.11	0.54 ± 0.09	0.81 ± 0.04	0.72 ± 0.05
MLP	0.55 ± 0.09	0.55 ± 0.07	0.78 ± 0.05	0.68 ± 0.06
Graph U-Net	0.54 ± 0.11	0.47 ± 0.2	0.74 ± 0.19	0.69 ± 0.12
GPST <sub>GINE</sub>	<b>0.6 ± 0.07</b>	0.54 ± 0.07	<b>0.84 ± 0.05</b>	<b>0.76 ± 0.06</b>
GTC	0.59 ± 0.09	<b>0.55 ± 0.11</b>	0.82 ± 0.06	0.73 ± 0.07
ChebyNet <sub>No LASSO</sub>	0.54 ± 0.08	0.52 ± 0.1	0.82 ± 0.06	0.75 ± 0.06
GAT <sub>No LASSO</sub>	0.54 ± 0.11	0.53 ± 0.14	0.69 ± 0.05	0.65 ± 0.07
GCN <sub>No LASSO</sub>	0.5 ± 0.09	0.43 ± 0.16	0.76 ± 0.03	0.7 ± 0.04
ChebyNet <sub>10 Layers</sub>	0.54 ± 0.08	0.52 ± 0.08	0.82 ± 0.05	0.74 ± 0.05
ChebyNet <sub>50 Layers</sub>	0.51 ± 0.09	0.49 ± 0.15	0.69 ± 0.08	0.61 ± 0.07
GAT <sub>10 Layers</sub>	0.49 ± 0.09	0.48 ± 0.08	0.67 ± 0.13	0.63 ± 0.14
GAT <sub>50 Layers</sub>	0.53 ± 0.09	0.51 ± 0.1	0.59 ± 0.07	0.51 ± 0.16
GCN <sub>10 Layers</sub>	0.55 ± 0.08	0.51 ± 0.09	0.69 ± 0.15	0.61 ± 0.12
ChebyNet <sub>random E</sub>	0.51 ± 0.15	0.46 ± 0.18	<b>0.84 ± 0.05</b>	0.74 ± 0.04
GAT <sub>random E</sub>	0.53 ± 0.07	0.53 ± 0.08	0.8 ± 0.07	0.7 ± 0.05
GCN <sub>random E</sub>	0.53 ± 0.09	0.49 ± 0.1	0.64 ± 0.13	0.6 ± 0.08
GPST <sub>random E</sub>	<b>0.59 ± 0.08</b>	<b>0.61 ± 0.05</b>	<b>0.84 ± 0.07</b>	<b>0.75 ± 0.06</b>
GTC <sub>random E</sub>	0.56 ± 0.09	0.55 ± 0.1	<b>0.84 ± 0.03</b>	0.73 ± 0.05

#### F. Biological Insights

Both SSN and MIN modeling pipelines identified genes and metabolites involved in the mitochondrial shuttle of acylcarnitines for fatty acid  $\beta$ -oxidation as relevant, including genes *SLC25A20* and *CPT1A*, and glutarylcarnitine (C5-DC). These preliminary findings align with previous work [23] [24] on associations between mitochondrial fatty acids and PD.

### IV. FUTURE WORK

We plan to further extract biological interpretations in the context of PD by identifying relevant molecular subnetworks and performing functional enrichment analysis. In addition, we will assess the statistical significance of our comparative analysis.

### ACKNOWLEDGEMENTS

We acknowledge support by Luxembourg’s National Research Fund (FNR) through the grants no. FNR/NCER13/BM/11264123 and C20/MS/14782078/QuaC, and the Marie Skłodowska-Curie grant agreement No. 764644.

## REFERENCES

- [1] M. M. Bronstein, J. Bruna, T. Cohen, and P. Veličković, "Geometric Deep Learning: Grids, Groups, Graphs, Geodesics, and Gauges," April 2021.
- [2] D. Duvenaud, D. Maclaurin, J. Aguilera-Iparraguirre, R. Gómez-Bombarelli, T. Hirzel, A. Aspuru-Guzik, and R. P. Adams, "Convolutional networks on graphs for learning molecular fingerprints," in *Advances in Neural Information Processing Systems*, vol. 2015-January, 2015.
- [3] M. Zitnik, M. Agrawal, and J. Leskovec, "Modeling polypharmacy side effects with graph convolutional networks," in *Bioinformatics*, vol. 34, 2018.
- [4] S. Itani and D. Thanou, "Combining anatomical and functional networks for neuropathology identification: A case study on autism spectrum disorder," *Medical Image Analysis*, vol. 69, 2021.
- [5] H. Chereda, A. Bleckmann, F. Kramer, A. Leha, and T. Beissbarth, "Utilizing molecular network information via graph convolutional neural networks to predict metastatic event in breast cancer," in *Studies in Health Technology and Informatics*, vol. 267, 2019.
- [6] H. Chereda, A. Bleckmann, K. Menck, J. Perera-Bel, P. Stegmaier, F. Auer, F. Kramer, A. Leha, and T. Beißbarth, "Explaining decisions of graph convolutional neural networks: patient-specific molecular subnetworks responsible for metastasis prediction in breast cancer," *Genome Medicine*, vol. 13, no. 1, 2021.
- [7] C. Yin, Y. Cao, P. Sun, H. Zhang, Z. Li, Y. Xu, and H. Sun, "Molecular Subtyping of Cancer Based on Robust Graph Neural Network and Multi-Omics Data Integration," *Frontiers in Genetics*, vol. 13, May 2022.
- [8] X. Li, J. Ma, L. Leng, M. Han, M. Li, F. He, and Y. Zhu, "MoGCN: A Multi-Omics Integration Method Based on Graph Convolutional Network for Cancer Subtype Analysis," *Frontiers in Genetics*, vol. 13, 2022.
- [9] T. Wang, W. Shao, Z. Huang, H. Tang, J. Zhang, Z. Ding, and K. Huang, "MOGONET integrates multi-omics data using graph convolutional networks allowing patient classification and biomarker identification," *Nature Communications*, vol. 12, no. 1, pp. 1–13, June 2021.
- [10] A. Conesa and S. Beck, "Making multi-omics data accessible to researchers," *Sci Data*, vol. 6, no. 1, p. 251, Oct. 2019.
- [11] Parkinson Progression Marker Initiative, "The Parkinson Progression Marker Initiative (PPMI)," *Prog Neurobiol*, vol. 95, no. 4, pp. 629-35, Dec. 2011.
- [12] G. Hipp et al., "The Luxembourg Parkinson's Study: A Comprehensive Approach for Stratification and Early Diagnosis," *Front Aging Neurosci*, vol. 10, 2018.
- [13] R. Tibshirani, "Regression shrinkage and selection via the lasso," *Journal of the Royal Statistical Society: Series B (Methodological)*, vol. 58, no. 1, pp. 267–288, 1996.
- [14] R. Ying, D. Bourgeois, J. You, M. Zitnik, and J. Leskovec, "GNExplainer: Generating explanations for graph neural networks," in *Advances in Neural Information Processing Systems*, vol. 32, 2019.
- [15] B. Malone, A. Garcia-Duran, and M. Niepert, "Learning Representations of Missing Data for Predicting Patient Outcomes," November 2018.
- [16] D. Szklarczyk, R. Kirsch, M. Koutrouli, K. Nastou, F. Mehryary, R. Hachilif, A. L. Gable, T. Fang, N. T. Doncheva, S. Pyysalo, P. Bork, L. J. Jensen, and C. Von Mering, "The STRING database in 2023: protein-protein association networks and functional enrichment analyses for any sequenced genome of interest," *Nucleic Acids Research*, vol. 51, no. 1 D, 2023.
- [17] D. Szklarczyk, A. Santos, C. Von Mering, L. J. Jensen, P. Bork, and M. Kuhn, "STITCH 5: augmenting protein–chemical interaction networks with tissue and affinity data," *Nucleic Acids Research*, vol. 44, no. Database issue, pp. D380, January 2016.
- [18] S. Haykin, *Neural Networks: A Comprehensive Foundation*, Prentice Hall PTR, 1994.
- [19] H. Gao and S. Ji, "Graph U-Nets," in *Proceedings of the 36th International Conference on Machine Learning*, PMLR 97:2083-2092, 2019.
- [20] L. Rampásek, M. Galkin, V. P. Dwivedi, A. T. Luu, G. Wolf, and D. Beaini, "Recipe for a general, powerful, scalable graph transformer," in *Proceedings of the 36th International Conference on Neural Information Processing Systems*, New Orleans, LA, USA, 2024, pp. 1054.
- [21] Y. Shi, Z. Huang, S. Feng, H. Zhong, W. Wang, and Y. Sun, "Masked Label Prediction: Unified Message Passing Model for Semi-Supervised Classification," in *Proceedings of the Thirtieth International Joint Conference on Artificial Intelligence, Main Track*, 2021, pp. 1548-1554.
- [22] A. F. Agarap, "Deep learning using rectified linear units (ReLU)," arXiv preprint arXiv:1803.08375, 2018.
- [23] D. Grassi, S. Howard, M. Zhou, N. Diaz-Perez, N. T. Urban, D. Guerrero-Given, N. Kamasawa, L. A. Volpicelli-Daley, P. LoGrasso, and C. I. Lasmézas, "Identification of a highly neurotoxic  $\alpha$ -synuclein species inducing mitochondrial damage and mitophagy in Parkinson's disease," *Proceedings of the National Academy of Sciences of the United States of America*, vol. 115, no. 11, 2018.
- [24] S. Saiki, T. Hatano, M. Fujimaki, K. I. Ishikawa, A. Mori, Y. Oji, A. Okuzumi, T. Fukuhara, T. Koinuma, Y. Imamichi, M. Nagumo, N. Furuya, S. Nojiri, T. Amo, K. Yamashiro, and N. Hattori, "Decreased long-chain

acylcarnitines from insufficient  $\beta$ -oxidation as potential early diagnostic markers for Parkinson's disease," *Scientific Reports*, vol. 7, no. 1, 2017.

## APPENDIX

### A. Data pre-processing

The transcriptomics data from PPMI was quantified by the STAR + featureCounts method, and, a low expression filter was applied, resulting in 23,253 features. Metabolomics data from the LuxPARK cohort were measured and initially pre-processed by Metabolon®, and the log-transformed batch normalized peak-area data was used. Since levodopa (L-DOPA) dopaminergic medication has a pronounced effect on the metabolism of blood, we additionally filtered out all metabolites from the data with a minimum absolute Pearson correlation of 0.2 with the L-DOPA metabolite 3-O-methyldopa (also known as 3-OMD or 3-methoxytyrosine) and all metabolites belonging to tyrosine metabolism and tryptophan metabolism prior to the analysis, resulting in 86 (5.77%) metabolites being eventually removed from the feature space.

Both datasets underwent unsupervised filtering (low-variance and highly correlated features were removed) prior to the sample-similarity network modelling pipeline, while transcriptomics data from the PPMI also underwent these unsupervised filters prior to the molecular interaction networks modelling to reduce the otherwise large feature space and mitigate a potential over-squashing effect after recursive aggregation of node features, creating a more compact and informative PPI network.

### B. Schemas of SSN and MIN modeling pipelines

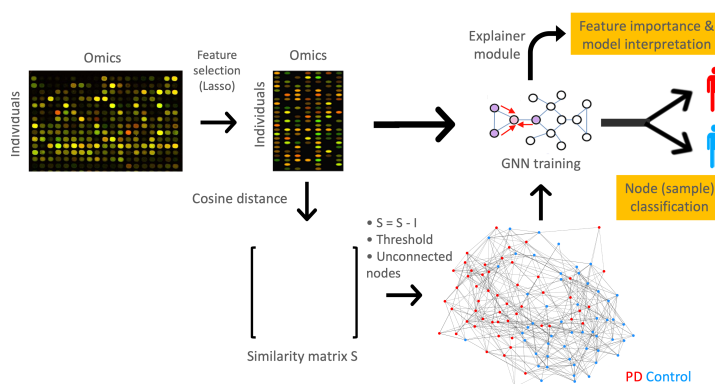


Fig. 1: Schema of graph representation learning using sample-sample similarity networks modeling pipeline.

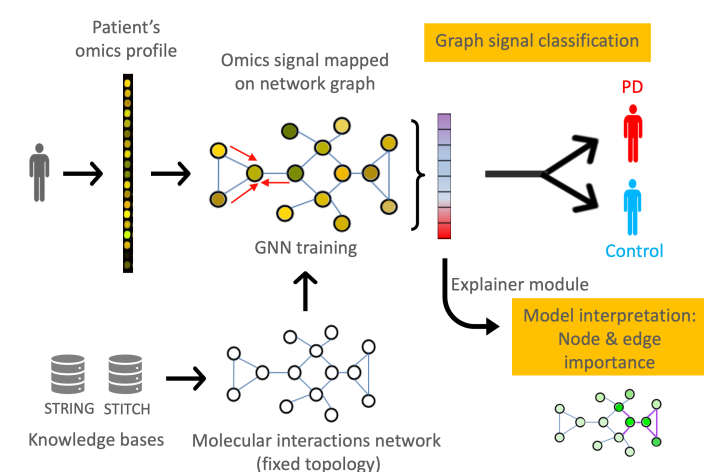


Fig. 2: Schema of graph representation learning using molecular interaction networks modeling pipeline.